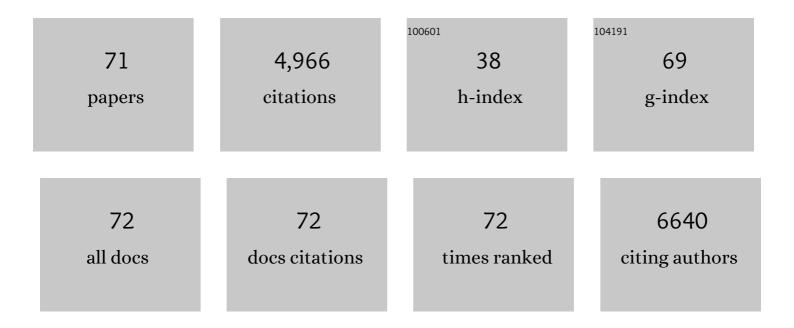
Yingguang Zhang

List of Publications by Year in descending order

Source: https://exaly.com/author-pdf/6961015/publications.pdf Version: 2024-02-01



#	Article	IF	CITATIONS
1	Photochemistry of Nitrate Ion: Reduction by Formic Acid under UV Irradiation. Photochemistry and Photobiology, 2022, 98, 404-411.	1.3	2
2	Multimetal tantalate CsBi2Ta5O16 for photocatalytic conversion of CO2 with H2O into CH4 and O2. Applied Surface Science, 2022, 588, 152933.	3.1	8
3	AuPd nanoparticle-decorated ultrathin Bi ₂ TiO ₄ F ₂ sheets for photocatalytic methane oxidation. New Journal of Chemistry, 2022, 46, 10545-10549.	1.4	1
4	Fabrication of 2H/3C-SiC heterophase junction nanocages for enhancing photocatalytic CO2 reduction. Journal of Colloid and Interface Science, 2022, 622, 31-39.	5.0	14
5	Photocatalytic Chlorination of Methane Using Alkali Chloride Solution. ACS Catalysis, 2022, 12, 7004-7013.	5.5	9
6	Sn ²⁺ and Cu ²⁺ Self-Codoped Cu ₂ ZnSnS ₄ Nanosheets Switching from p-Type to n-Type Semiconductors for Visible-Light-Driven CO ₂ Reduction. ACS Sustainable Chemistry and Engineering, 2022, 10, 8825-8834.	3.2	9
7	Intimately Contacted Ni2P on CdS Nanorods for Highly Efficient Photocatalytic H2 Evolution: New Phosphidation Route and the Interfacial Separation Mechanism of Charge Carriers. Applied Catalysis B: Environmental, 2021, 281, 119443.	10.8	90
8	Enhanced bacterial disinfection by CuI–BiOI/rGO hydrogel under visible light irradiation. RSC Advances, 2021, 11, 20446-20456.	1.7	11
9	Monolayer Bi ₂ W _{1–<i>x</i>} Mo <i>_x</i> O ₆ Solid Solutions for Structural Polarity to Boost Photocatalytic Reduction of Nitrobenzene under Visible Light. ACS Sustainable Chemistry and Engineering, 2021, 9, 2465-2474.	3.2	32
10	Metallic Pt and PtO ₂ Dual-Cocatalyst-Loaded Binary Composite RGO-CN <i>_x</i> for the Photocatalytic Production of Hydrogen and Hydrogen Peroxide. ACS Sustainable Chemistry and Engineering, 2021, 9, 6380-6389.	3.2	29
11	Distortion of the Coordination Structure and High Symmetry of the Crystal Structure in In ₄ SnS ₈ Microflowers for Enhancing Visible-Light Photocatalytic CO ₂ Reduction. ACS Catalysis, 2021, 11, 11029-11039.	5.5	37
12	Construction of the Rutile/Anatase Micro-Heterophase Junction Photocatalyst from Anatase by Liquid Nitrogen Quenching Method. ACS Applied Energy Materials, 2021, 4, 10172-10186.	2.5	9
13	Controlling 1T/2H heterophase junctions in the MoS ₂ microsphere for the highly efficient photocatalytic hydrogen evolution. Catalysis Science and Technology, 2021, 11, 7914-7921.	2.1	4
14	Photocatalytic reduction of CO2 on BiOX: Effect of halogen element type and surface oxygen vacancy mediated mechanism. Applied Catalysis B: Environmental, 2020, 274, 119063.	10.8	243
15	Direct and indirect Z-scheme heterostructure-coupled photosystem enabling cooperation of CO2 reduction and H2O oxidation. Nature Communications, 2020, 11, 3043.	5.8	200
16	Mechanistic insights into toluene degradation under VUV irradiation coupled with photocatalytic oxidation. Journal of Hazardous Materials, 2020, 399, 122967.	6.5	48
17	Integrating single Ni sites into biomimetic networks of covalent organic frameworks for selective photoreduction of CO ₂ . Chemical Science, 2020, 11, 6915-6922.	3.7	78
18	BiVO4 /Bi4Ti3O12 heterojunction enabling efficient photocatalytic reduction of CO2 with H2O to CH3OH and CO. Applied Catalysis B: Environmental, 2020, 270, 118876.	10.8	179

YINGGUANG ZHANG

#	Article	IF	CITATIONS
19	Regulation of the rutile/anatase TiO ₂ heterophase interface by Ni ₁₂ P ₅ to improve photocatalytic hydrogen evolution. Catalysis Science and Technology, 2020, 10, 3709-3719.	2.1	18
20	Understanding structure-function relationships in HZSM-5 zeolite catalysts for photocatalytic oxidation of isopropyl alcohol. Journal of Catalysis, 2019, 377, 322-331.	3.1	21
21	Ranking the relative CO2 electrochemical reduction activity in carbon materials. Carbon, 2019, 154, 108-114.	5.4	14
22	A low-cost and dendrite-free rechargeable aluminium-ion battery with superior performance. Journal of Materials Chemistry A, 2019, 7, 17420-17425.	5.2	111
23	Non-noble metal thickness-tunable Bi2MoO6 nanosheets for highly efficient visible-light-driven nitrobenzene reduction into aniline. Applied Catalysis B: Environmental, 2019, 259, 118087.	10.8	80
24	<i>In situ</i> hydrothermal etching fabrication of CaTiO ₃ on TiO ₂ nanosheets with heterojunction effects to enhance CO ₂ adsorption and photocatalytic reduction. Catalysis Science and Technology, 2019, 9, 336-346.	2.1	56
25	One-step green conversion of benzyl bromide to aldehydes on NaOH-modified g-C ₃ N ₄ with dioxygen under LED visible light. Catalysis Science and Technology, 2019, 9, 3270-3278.	2.1	15
26	Synthesis of caged iodine-modified ZnO nanomaterials and study on their visible light photocatalytic antibacterial properties. Applied Catalysis B: Environmental, 2019, 256, 117873.	10.8	79
27	Plasmonic control of solar-driven CO2 conversion at the metal/ZnO interfaces. Applied Catalysis B: Environmental, 2019, 256, 117823.	10.8	95
28	Defect engineering of metal–oxide interface for proximity of photooxidation and photoreduction. Proceedings of the National Academy of Sciences of the United States of America, 2019, 116, 10232-10237.	3.3	63
29	Roomâ€Temperature Activation of H ₂ by a Surface Frustrated Lewis Pair. Angewandte Chemie - International Edition, 2019, 58, 9501-9505.	7.2	72
30	The effect of excitation wavelength on the photodeposition of Pt on polyhedron BiVO4 with exposing {010} and {110} facets for photocatalytic performance. Catalysis Communications, 2019, 123, 100-104.	1.6	10
31	Highâ€Rate, Tunable Syngas Production with Artificial Photosynthetic Cells. Angewandte Chemie, 2019, 131, 7800-7804.	1.6	12
32	Highâ€Rate, Tunable Syngas Production with Artificial Photosynthetic Cells. Angewandte Chemie - International Edition, 2019, 58, 7718-7722.	7.2	75
33	Reconstructing Dualâ€Induced {0 0 1} Facets Bismuth Oxychloride Nanosheets Heterostructures: An Effective Strategy to Promote Photocatalytic Oxygen Evolution. Solar Rrl, 2019, 3, 1900059.	3.1	44
34	More efficiently enhancing photocatalytic activity by embedding Pt within anatase–rutile TiO2 heterophase junction than exposing Pt on the outside surface. Journal of Catalysis, 2019, 372, 8-18.	3.1	37
35	Roomâ€Temperature Activation of H ₂ by a Surface Frustrated Lewis Pair. Angewandte Chemie, 2019, 131, 9601-9605.	1.6	18
36	Persian buttercup-like BiOBrxCl1-x solid solution for photocatalytic overall CO2 reduction to CO and O2. Applied Catalysis B: Environmental, 2019, 243, 734-740.	10.8	159

YINGGUANG ZHANG

#	Article	IF	CITATIONS
37	Amorphous Ta2OxNy-enwrapped TiO2 rutile nanorods for enhanced solar photoelectrochemical water splitting. Applied Catalysis B: Environmental, 2019, 243, 481-489.	10.8	86
38	In situ constructing interfacial contact MoS2/ZnIn2S4 heterostructure for enhancing solar photocatalytic hydrogen evolution. Applied Catalysis B: Environmental, 2018, 233, 112-119.	10.8	181
39	MnSb ₂ S ₄ Monolayer as an Anode Material for Metal-Ion Batteries. Chemistry of Materials, 2018, 30, 3208-3214.	3.2	74
40	Rapid water disinfection over a Ag/AgBr/covalent triazine-based framework composite under visible light. Dalton Transactions, 2018, 47, 7077-7082.	1.6	24
41	PdSn/NiO/NaTaO3:La for photocatalytic ammonia synthesis by reduction of NO3â^' with formic acid in aqueous solution. Journal of Catalysis, 2018, 361, 303-312.	3.1	45
42	Oxygen vacancy modulation of two-dimensional γ-Ga ₂ O ₃ nanosheets as efficient catalysts for photocatalytic hydrogen evolution. Nanoscale, 2018, 10, 21509-21517.	2.8	31
43	Phase Transition of Two-Dimensional β-Ga ₂ O ₃ Nanosheets from Ultrathin γ-Ga ₂ O ₃ Nanosheets and Their Photocatalytic Hydrogen Evolution Activities. ACS Omega, 2018, 3, 14469-14476.	1.6	40
44	Visible-Light Driven Overall Conversion of CO ₂ and H ₂ O to CH ₄ and O ₂ on 3D-SiC@2D-MoS ₂ Heterostructure. Journal of the American Chemical Society, 2018, 140, 14595-14598.	6.6	361
45	The effect of halogen on BiOX (X = Cl, Br, I)/Bi2WO6 heterojunction for visible-light-driven photocatalytic benzyl alcohol selective oxidation. Applied Catalysis A: General, 2018, 567, 65-72.	2.2	75
46	Surface oxygen vacancy and defect engineering of WO ₃ for improved visible light photocatalytic performance. Catalysis Science and Technology, 2018, 8, 4399-4406.	2.1	158
47	Cul-BiOI/Cu film for enhanced photo-induced charge separation and visible-light antibacterial activity. Applied Catalysis B: Environmental, 2018, 235, 238-245.	10.8	85
48	Simple Fabrication of SnO ₂ Quantumâ€dotâ€modified TiO ₂ Nanorod Arrays with High Photoelectrocatalytic Activity for Overall Water Splitting. ChemPhysChem, 2018, 19, 2717-2723.	1.0	16
49	Openmouthed β-SiC hollow-sphere with highly photocatalytic activity for reduction of CO2 with H2O. Applied Catalysis B: Environmental, 2017, 206, 158-167.	10.8	79
50	Controllable synthesis of Bi2WO6 nanoplate self-assembled hierarchical erythrocyte microspheres via a one-pot hydrothermal reaction with enhanced visible light photocatalytic activity. Applied Surface Science, 2017, 403, 326-334.	3.1	46
51	Freestanding single layers of non-layered material γ-Ga ₂ O ₃ as an efficient photocatalyst for overall water splitting. Journal of Materials Chemistry A, 2017, 5, 9702-9708.	5.2	46
52	Heterojunction: important strategy for constructing composite photocatalysts. Science Bulletin, 2017, 62, 599-601.	4.3	57
53	In situ construction of a heterojunction over the surface of a sandwich structure semiconductor for highly efficient photocatalytic H ₂ evolution under visible light irradiation. Nanoscale, 2017, 9, 14423-14430.	2.8	15
54	Photocatalytic reduction of CO2 to CO over the Ti–Highly dispersed HZSM-5 zeolite containing Fe. Applied Catalysis B: Environmental, 2017, 203, 725-730.	10.8	44

YINGGUANG ZHANG

#	Article	IF	CITATIONS
55	Post-synthetic regulation of the structure, morphology and photoactivity of graphitic carbon nitride by heat-vacuum treatment. Materials and Design, 2017, 114, 208-213.	3.3	7
56	Synergy of metal and nonmetal dopants for visible-light photocatalysis: a case-study of Sn and N co-doped TiO ₂ . Physical Chemistry Chemical Physics, 2016, 18, 9636-9644.	1.3	68
57	HZSM-5 zeolites containing impurity iron species for the photocatalytic reduction of CO ₂ with H ₂ O. Catalysis Science and Technology, 2016, 6, 7579-7585.	2.1	33
58	One-step synthesis of mesoporous Pt–Nb ₂ O ₅ nanocomposites with enhanced photocatalytic hydrogen production activity. RSC Advances, 2016, 6, 96809-96815.	1.7	20
59	Large-scale preparation of heterometallic chalcogenide MnSb ₂ S ₄ monolayer nanosheets with a high visible-light photocatalytic activity for H ₂ evolution. Chemical Communications, 2016, 52, 13381-13384.	2.2	18
60	Simultaneous excitation of PdCl2 hybrid mesoporous g-C3N4 molecular/solid-state photocatalysts for enhancing the visible-light-induced oxidative removal of nitrogen oxides. Applied Catalysis B: Environmental, 2016, 184, 174-181.	10.8	39
61	Trace Amount of SnO ₂ -Decorated ZnSn(OH) ₆ as Highly Efficient Photocatalyst for Decomposition of Gaseous Benzene: Synthesis, Photocatalytic Activity, and the Unrevealed Synergistic Effect between ZnSn(OH) ₆ and SnO ₂ . ACS Catalysis, 2016. 6. 957-968.	5.5	74
62	Ultrathin nanosheets of molecular sieve SAPO-5: A new photocatalyst for efficient photocatalytic reduction of CO 2 with H 2 O to methane. Applied Catalysis B: Environmental, 2016, 187, 11-18.	10.8	62
63	Robust Photocatalytic H2O2 Production by Octahedral Cd3(C3N3S3)2 Coordination Polymer under Visible Light. Scientific Reports, 2015, 5, 16947.	1.6	71
64	Interim Anatase Coating Layer Stabilizes Rutile@Cr _{<i>x</i>} O _{<i>y</i>} Photoanode for Visible‣ightâ€Driven Water Oxidation. ChemPhysChem, 2015, 16, 1352-1355.	1.0	8
65	Towards a comprehensive insight into efficient hydrogen production by self-assembled Ru(bpy) ₃ ²⁺ –polymer–Pt artificial photosystems. Physical Chemistry Chemical Physics, 2015, 17, 10726-10736.	1.3	15
66	Enhanced visible-light-driven photocatalytic removal of NO: Effect on layer distortion on g-C3N4 by H2 heating. Applied Catalysis B: Environmental, 2015, 179, 106-112.	10.8	131
67	Monolayered Bi2WO6 nanosheets mimicking heterojunction interface with open surfaces for photocatalysis. Nature Communications, 2015, 6, 8340.	5.8	578
68	Vacuum heat-treatment of carbon nitride for enhancing photocatalytic hydrogen evolution. Journal of Materials Chemistry A, 2014, 2, 17797-17807.	5.2	94
69	Layered C ₃ N ₃ S ₃ Polymer/Graphene Hybrids as Metal-Free Catalysts for Selective Photocatalytic Oxidation of Benzylic Alcohols under Visible Light. ACS Catalysis, 2014, 4, 3302-3306.	5.5	89
70	Probing the Electronic Structure and Photoactivation Process of Nitrogenâ€Đoped TiO ₂ Using DRS, PL, and EPR. ChemPhysChem, 2012, 13, 1542-1550.	1.0	29
71	Nitrogen-doped titanium dioxide visible light photocatalyst: Spectroscopic identification of photoactive centers. Journal of Catalysis, 2010, 276, 201-214.	3.1	185